Comparative Analysis of EGGN vs. GGN Models for Hybrid Raman/DFA Amplified Ultra-Wideband Optical Networks

M.Mehrabi¹, F.Arpanaei^{2*}, M.Ranjbar Zefreh³, H.Beyranvand¹, M.Javad Emadi¹, P.Mahdizadeh¹, C.Natalino⁴, José M. Rivas-Moscoso⁵, Ó. González de Dios⁵, Juan P. Fernández-Palacios⁵, D. Larrabeiti², and J.Alberto Hernández²

Department of Electrical Engineering, Amirkabir University of Technology (Tehran Polytechnic), Tehran, Iran,
 Department of Telematic Engineering, Universidad Carlos III de Madrid, 28911 Leganes, Madrid, Spain,
 CISCO Systems S.R.L., Vimercate (MB), Italy, ⁴Department of Electrical Engineering, Chalmers University of Technology, 41296 Gothenburg, Sweden, ⁵Telefónica Research and Development, Madrid, Spain.

*farhad.arpanaei@uc3m.es

ABSTRACT

This paper presents a comparative analysis of the Enhanced Gaussian Noise (EGGN) and Gaussian Noise (GGN) models for estimating nonlinear interference (NLI) in hybrid Raman/doped fiber amplifier (DFA)-based ultra-wideband optical networks. Results demonstrate that the EGGN model achieves a significant 2.6 dB improvement in GSNR compared to the GGN model. Furthermore, the study utilizes an analytical solution to compute the NLI, reducing computation time from 7.5 hours to 2 minutes. These findings highlight the benefits of the EGGN model and the efficiency of the analytical approach for accurate and rapid performance assessment of ultra-wideband optical systems.

Keywords: GGN; EGGN; ultra-wideband; Optical Networks; nonlinear interference; hybrid Raman/DFA amplifiers.

1. INTRODUCTION

The continuous growth in data traffic pressures vendors to extend optical transmission beyond the C-band, utilizing the entire low-loss optical spectrum of single-mode fibers (SMFs), called ultra-wideband optical networks. Beyond the C-band networks, the channels operating in the L-, S-, E-, U-, and O-bands experience considerable attenuation due to the power transfer associated with the inter-channel stimulated Raman scattering (ISRS) effect. This attenuation cannot be sufficiently compensated for only using Doped Fiber Amplifiers (DFAs) [1]. To address this challenge, hybrid Raman/DFA amplification can be adopted, which allows the deployment of discrete and distributed Raman amplifiers in co-propagating and counter-propagating directions, in conjunction with DFAs. This strategy enables achieving any desired gain by adjusting the power and frequency of the Raman pumps while achieving a reduced noise figure [2,3]. In resource allocation based on quality of transmission (QoT), the generalized signal-to-noise ratio (GSNR) of lightpaths must be calculated, which involves calculating amplified spontaneous emission (ASE) and non-linear interference (NLI) noises [4]. Furthermore, various methodologies for accurate prediction of GSNR have been introduced in the literature, e.g., simple fully loaded and low marginal predictions. These methods can be employed particularly in the migration from C-band to ultra-wideband networks [5].

Hybrid Raman/DFA amplification is essential for enabling efficient and scalable ultra-wideband networks [6]. The combination of Raman and DFA technologies offers significant advantages, including extended reach, improved signal quality, and higher capacity [7]. Raman amplifiers provide distributed gain along the fiber, reducing noise accumulation and mitigating non-linear effects, while DFAs deliver high output power and flat gain profiles over a broad wavelength range. By leveraging the strengths of both amplifiers, hybrid solutions ensure optimal performance for multi-band optical networks, supporting high data rates, long-distance transmission, and spectral efficiency [6]. This approach is crucial for next-generation networks, where multi-band operation is necessary to meet the growing demand for capacity and flexibility [7]. In a hybrid Raman/DFA amplification context, the ASE noise is determined by solving a set of coupled ordinary differential equations (ODEs) [8]. Regarding NLI noise, two primary models exist in the literature: the generalized Gaussian noise model (GGN) applicable to Gaussian signals [9], and the enhanced GGN model with Raman support (EGGN) which incorporates a correction term for non-Gaussian modulation formats [10]. In addition to these integral-based models, the authors in [11,12] developed closed-form expressions for the NLI noise in the presence of Raman amplification.

This work investigates the hybrid Raman/DFA amplified S+C+L-band optical networks. We study the accuracy of the NLI values when employing the EGGN model instead of the GGN. In this work, to ensure a fair comparison,

the closed-forms of [11, 12] are not evaluated against the integral-based GGN and EGGN models. Furthermore, two approaches for computing the z-domain integral of the link function are examined; the numerical approach utilized by the cutting-edge Gaussian Noise in Python (GNPy) project [13], and the analytical approach introduced in [14]. Since the NLI model presented in [14] is validated through experiments in [15], we consider it the ground truth NLI value. The findings show that the SNR_{NLI} derived from the EGGN model is more accurate than that obtained from the GGN, up to 7.5 dB. Furthermore, the SNR_{NLI} obtained by the GNPy exhibit lower accuracy up to 9.2 dB compared to the values obtained by [14] when considering the GGN model. Additionally, the analytical solution of the z-domain NLI integral improves the processing speed up to 200 times compared to the numerical computation.

2. System Model

We consider $N_{\rm ch}$ optical channels over the S+C+L-band, propagating in the +z direction through a single-span link. Furthermore, a distributed Raman amplifier including N_p backward pumps, which propagate in the -z direction, is located at the end of the span. The remaining loss of the channels is compensated by employing Erbium- and Thallium-DFAs (EDFA and TDFA) for the C-/L-band and S-band channels, respectively, after the Raman pumps. The power profile of the channels and pumps can be modeled by a set of coupled ODEs as [8]:

$$\frac{\partial S(f_{i},z)}{\partial z} = \left\{ \sum_{j=1}^{N_{\text{ch}}} \Upsilon\left(\frac{f_{i}}{f_{j}}\right) C_{i,j} S(f_{j},z) + \sum_{k=1}^{N_{p}} \Upsilon\left(\frac{f_{i}}{f_{k}}\right) C_{i,k} P(f_{k},z) - \alpha(f_{i}) \right\} S(f_{i},z); \qquad i \in \{1,2,...,N_{\text{ch}}\},$$

$$-\frac{\partial P(f_{l},z)}{\partial z} = \left\{ \sum_{j=1}^{N_{\text{ch}}} \Upsilon\left(\frac{f_{l}}{f_{j}}\right) C_{l,j} S(f_{j},z) + \sum_{k=1}^{N_{p}} \Upsilon\left(\frac{f_{l}}{f_{k}}\right) C_{l,k} P(f_{k},z) - \alpha(f_{l}) \right\} P(f_{l},z); \qquad l \in \{1,2,...,N_{p}\},$$

$$(1)$$

where $S(f_i, z)$ denotes the power of channel i with center frequency f_i at distance z, while $P(f_i, z)$ represents the power of the pump at frequency f_i . $\alpha(f_i)$ indicates the fiber attenuation at frequency f_i , and $C_{i,j}$ is the polarization-averaged Raman gain coefficient, normalized by the effective core area, for a frequency separation $\Delta f = |f_i - f_j|$. The function $\Upsilon(x)$ returns -x for x > 1, 0 for x = 1, and 1 for x < 1. The Raman amplifier-induced ASE noise within the bandwidth of channel i, denoted as $P_{\text{ASE,R}}(f_i, z)$, is characterized through ODEs as [8]:

$$\frac{\partial P_{\text{ASE,R}}(f_i,z)}{\partial z} = \left\{ \sum_{j=1}^{N_{\text{ch}}} \Upsilon\left(\frac{f_i}{f_j}\right) C_{i,j} S(f_j,z) + \sum_{k=1}^{N_p} \Upsilon\left(\frac{f_i}{f_k}\right) C_{i,k} P(f_k,z) - \alpha(f_i) \right\} P_{\text{ASE,R}}(f_i,z) \\
+ \left\{ \sum_{j=1}^{N_{\text{ch}}} \eta_{i,j} \Upsilon\left(\frac{f_i}{f_j}\right) C_{i,j} S(f_j,z) + \sum_{k=1}^{N_p} \eta_{i,k} \Upsilon\left(\frac{f_i}{f_k}\right) C_{i,k} P(f_k,z) \right\} 2h f_i B_i; \quad i \in \{1,2,...,N_{\text{ch}}\},$$
(2)

where B_i is the bandwidth of channel i, $\eta_{i,j} = 1 + H_{i,j}$, and $H_{i,j} = \left(exp\left[\frac{h\Delta f}{k_BT}\right] - 1\right)^{-1}$ shows the mean number of photons in a normal node. h, k_B , and T are Planck's constant, Boltzmann's constant, and fiber temperature, respectively. In the hybrid Raman/DFA amplification context, at the end of the span with length L_s , the ASE noise of $P_{\text{ASE},R}(f_i,z)|_{z=L_s}$ is amplified by the EDFA/TDFA, which provides the ideal gain G_i . Thus, the total ASE noise is derived by $P_{\text{ASE},R}(f_i) = G_i P_{\text{ASE},R}(f_i,z)|_{z=L_s} + 2(G_i-1)n_{\text{sp}}hf_iB_i$, where n_{sp} is the spontaneous emission factor.

The GGN model to calculate the NLI noise is described by an integral formulation as [9]:

$$G_{\text{NLI}}^{\text{GGN}}(f) = \frac{16}{27} \gamma^2 \iint_{-\infty}^{+\infty} G_{\text{TX}}(f_1) G_{\text{TX}}(f_2) G_{\text{TX}}(f_1 + f_2 - f) |\mu(f_1, f_2, f)|^2 df_1 df_2, \tag{3}$$

where $\mu(f_1,f_2,f)=\int_0^{L_s} exp\left(j4\pi^2(f_1-f)(f_2-f)\left[\beta_2+\pi\beta_3(f_1+f_2)\right]\zeta\right)\frac{\rho(\zeta,f_1)\rho(\zeta,f_1+f_2-f)\rho(\zeta,f_2)}{\rho(\zeta,f)}d\zeta$ refers to the link function, $\rho(z,f)$ denotes the normalized amplitude profile, and $G_{\rm TX}(f)$ represents the transmitted power spectral density of the channel with center frequency f. Additionally, γ , β_2 , and β_3 are the fiber's nonlinear coefficient, dispersion, and dispersion slope, respectively. Calculating the link function $\mu(f_1,f_2,f)$, which also appears in the correction terms introduced by the EGGN model, is a significant component of the NLI noise computation. This work studies two approaches for calculating the link function $\mu(f_1,f_2,f)$ within the hybrid Raman/DFA amplification context. The first method is called the numerical link function (NLF) approach, which employs the technique of *integration by parts*, similar to the approach utilized by the GNPy. The second method is named the analytical link function (ALF) approach, which incorporates a *finite degree polynomial representation* as introduced in [14]. The subsequent section examines the accuracy and processing speed of these approaches.

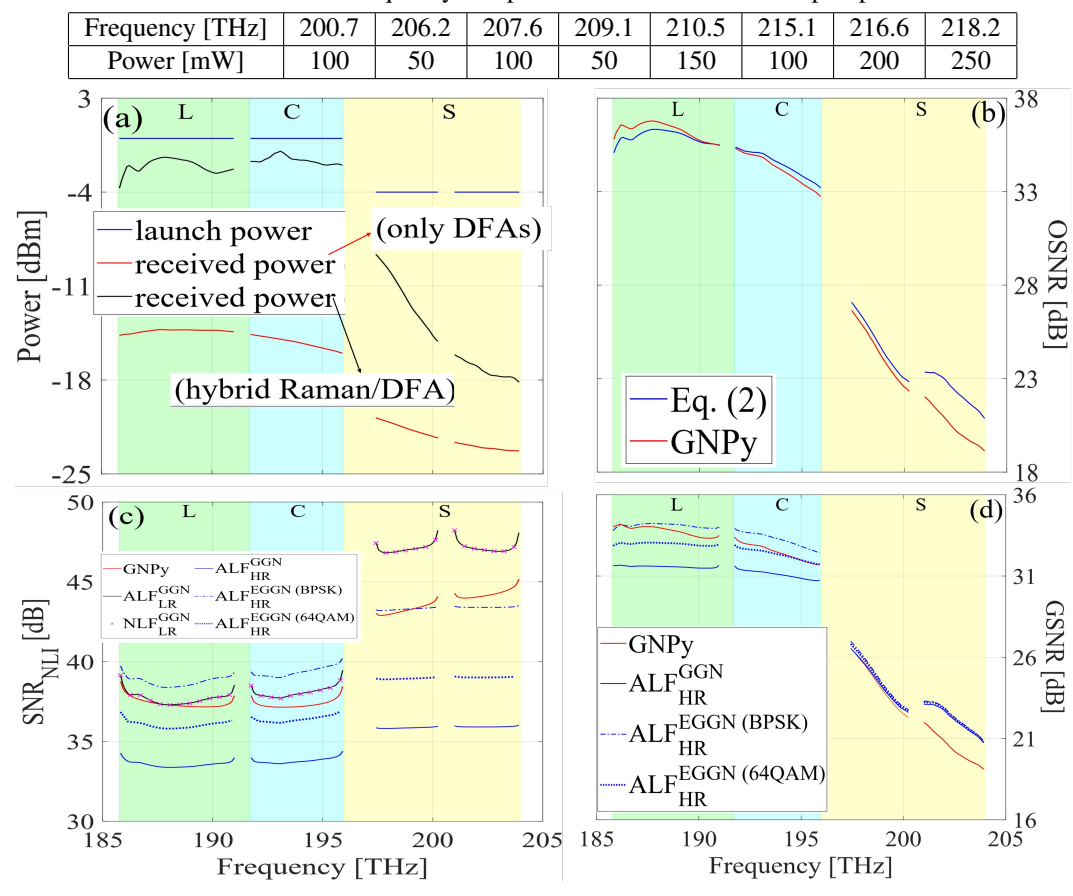


Table 1: The frequency and power of considered Raman pumps

Fig. 1: The (a) power profiles, (b) OSNR, (c) SNR_{NLI}, and (d) GSNR of channels over S+C+L-band.

3. Simulations Setup, Numerical Results, and Conclusion

In this paper, we study a fully loaded S+C+L-band optical network consisting of $N_{\rm ch}$ =138 channels, each modulated at a symbol rate of 100 GBd. The channels are spaced by 112.5 GHz and are centered at 1540 nm. Furthermore, 5 and 10 nm spectral guard bands are incorporated between the C- and L-bands, and the S- and C-bands, respectively. The launch power of the channels in the C-/L- bands and S-band are set at 0 and -4 dBm, respectively. In the hybrid Raman/DFA amplification context for a point-to-point transmission over a single 80 km standard SMF span, we consider eight backward Raman pumps as detailed in Table 1 [11, 12]. Moreover, DFAs are employed to recover the launch power of the signals at the end of the span. The average noise figures for the L- and C-band EDFAs are 6 and 5.5 dB, respectively, while the S-band TDFA exhibits an average noise figure of 7 dB. Results are derived through the GNPy, NLF, and ALF approaches, considering the GGN model. The polarization multiplexed-binary phase shift keying (PM-BPSK) and -64 quadrature amplitude modulation (PM-64QAM) modulation formats within the EGGN model are applied to the ALF approach. Additionally, the low- and high-resolution (LR and HR) solutions of the f-domain integrals existing in (3) are analyzed.

Let us define $GSNR(f_i) = [OSNR^{-1}(f_i) + SNR_{NLI}^{-1}(f_i)]^{-1}$, where $OSNR(f_i) = S(f_i, 0)/P_{ASE}(f_i)$, and $SNR_{NLI}(f_i) = S(f_i, 0)/P_{NLI}(f_i)$. Moreover, $S(f_i, 0)$ and $P_{NLI}(f_i)$ are the launch power and the NLI power of the channel with center frequency f_i , respectively. Fig.1(a) illustrates the received powers with and without using Raman amplifiers across all channels. When Raman pumps are not employed, the S-band channels exhibit significant losses, reaching as high as 19.29 dB. Conversely, when Raman pumps are utilized, between 27% and 93% of these losses can be mitigated. In the computation of $P_{ASE,R}(f_i,z)$, the GNPy considers only the ASE noises generated by the pumps operating at frequencies exceeding f_i , while neglecting the ASE noises from other pumps and channels. Thus, as shown in Fig.1(b), the OSNR

values calculated by the GNPy exhibit some inaccuracies, particularly up to 2.1 dB concerning the S-band channels with center frequencies exceeding the Raman pump at 200.7 THz. Fig.1(c) shows the SNR_{NLI} values obtained by different approaches. In this figure, the superscripts indicate the GGN/EGGN model, while the subscripts demonstrate the LR/HR solutions of (3). According to this figure, both the ALF_{LR}^{GGN} and NLF_{LR}^{GGN} approaches exhibit similar accuracy in the SNR_{NLI} calculation. However, the runtime of the ALF is about 2 minutes, whereas the NLF requires 7.5 hours to derive the results. These approaches are simulated on a computer with an Intel Core i9-9900K and 32 GB of RAM. Thus, HR solutions are exclusively obtained through the ALF approach. Furthermore, this figure illustrates that the SNR_{NLI} values obtained from the GNPy fall within the range established by the ALF_{LR}^{GGN} and ALF_{HR}^{GGN} approaches. This indicates that the GNPy exhibits a lower accuracy than the ALF_{HR}^{GGN} approach, with a discrepancy of up to 9.2 dB. The other finding drawn from this figure indicates that utilizing the $ALF_{HR}^{EGGN (BPSK)}$ approach, which incorporates the EGGN model, enhances the accuracy of the calculated SNR_{NLI} up to 7.5 dB in comparison to the ALF_{HR}^{GGN} approach. As illustrated in Fig.1(d), the GSNR values derived by the GNPy and ALF approach exhibit discrepancies attributed to differences in the OSNR and SNR_{NLI} values. The GSNR values of the ALF approach are derived by utilizing (2) in OSNR calculations. According to this figure, the GSNR computed using the ALF_{HR} approach demonstrates superior accuracy compared to the GNPy, with an improvement of 2.5 dB. Moreover, employing the EGGN model instead of the GGN further increases the accuracy of the ALF approach by as much as 2.6 dB. In conclusion, the simulation results of hybrid Raman/DFA amplified S+C+L-band optical networks indicate that up to 7.5 dB accuracy enhancement in the SNR_{NLI} values can be achieved by utilizing the EGGN model instead of the GGN. Moreover, the ALF approach improves the accuracy of the GSNR estimation by as much as 2.5 dB compared to the GNPy.

4. Conclusions

This study demonstrates the superior accuracy of the EGGN model for estimating nonlinear interference in hybrid Raman/DFA amplified ultra-wideband optical networks. The EGGN model achieves a significant improvement in NLI compared to the GGN model. Furthermore, the analytical approach to computing the NLI integral offers a dramatic reduction in computation time, enabling faster and more efficient design and optimization of these complex optical systems. These findings suggest that the EGGN model, coupled with the analytical solution, is a valuable tool for accurately predicting and mitigating the impact of nonlinearities in future ultra-wideband deployments.

ACKNOWLEDGEMENTS

The authors would like to acknowledge the support of the EU-funded SEASON project (grant No. 101096909) and FLEX-SCALE project (grant No. 101092766), and Spanish funded Fun4date-Redes project (grant No.PID2022-136684OBC21).

References

- 1. Andrea D'Amico et al. Scalable and disaggregated GGN approximation applied to a C+L+S optical network. JLT, 2022.
- 2. Jing Chen et al. Optimal design of gain-flattened raman fiber amplifiers using a hybrid approach combining randomized neural networks and differential evolution algorithm. *IEEE Photonics Journal*, 2018.
- 3. Darko Zibar et al. Inverse system design using machine learning: The Raman amplifier case. JLT, 2020.
- Farhad Arpanaei et al. Synergizing hyper-accelerated power optimization and wavelength-dependent qot-aware cross-layer design in next-generation multi-band eons. IEEE JSAC, pages 1–1, 2025.
- Mahdieh Mehrabi et al. Efficient statistical qot-aware resource allocation in eons over the c+l-band: a multi-period and low-margin perspective. JOCN, 16(5):577-592, 2024.
- 6. Andre Souza et al. Raman amplifier design and launch power optimization in multi-band optical systems. JOCN, 17(1):A13-A22, 2025.
- 7. Lutz Rapp. Challenges for multiband optical amplification and solutions therefore. JLT, 42(12):4202-4212, 2024.
- 8. Wei Wang et al. Amplified spontaneous emission and rayleigh scattering in few-mode fiber raman amplifiers. *IEEE Photonics Technology Letters*, 2017.
- 9. Mattia Cantono et al. On the interplay of nonlinear interference generation with stimulated Raman scattering for QoT estimation. *JLT*, 2018.
- 10. Andrea Carena et al. EGN model of non-linear fiber propagation. Opt. Express, 2014.
- H. Buglia et al. A modulation-format dependent closed-form expression for the Gaussian noise model in the presence of Raman amplification. In ECOC, 2023.
- 12. Henrique Buglia et al. A closed-form expression for the Gaussian noise model in the presence of Raman amplification. JLT, 2024.
- 13. Alessio Ferrari et al. GNPy: an open source application for physical layer aware open optical networks. JOCN, 2020.
- 14. Mahdi Ranjbar Zefreh et al. Characterization of the link function in GN and EGN methods for nonlinearity assessment of ultrawideband coherent fiber optic communication systems with Raman effect, 2020. arXiv:2009.12687.
- 15. Yanchao Jiang et al. Closed-form EGN model with comprehensive Raman support. [Paper presentation]. ECOC, 2024.